Wave Functions at the Critical Kolmogorov-Arnol'd-Moser Surface

Günter Radons

Institut für Theoretische Physik, Universität Kiel, 2300 Kiel, Federal Republic of Germany

and

R. E. Prange

Department of Physics, University of Maryland, College Park, Maryland 20742

(Received 10 May 1988)

A quantum system whose classical limit is at the critical threshold to global chaos is studied, i.e., in the small Planck's constant limit the last invariant torus is about to disappear. The quantum states are compared with classical phase-space structure near this torus. We exhibit the extension of the scaling properties of the latter to the quantum regime and find a new scaling of the quantum eigenvalues.

We exhibit here quantum eigenstates corresponding to classical orbits near a critical Kolmogorov-Arnol'd-Moser (KAM) surface. The dissolution of the last KAM torus (into a cantorus) as a parameter, κ, reaches a critical value, κ_c, signals the onset of global stochastic diffusion. This effect is observed at the onset of many-proton ionization in Rydberg hydrogen as the amplitude of the driving microwave field surpasses a critical value,[1] and so it is clear that an understanding of related quantum effects is necessary. Other problems such as dissociation in molecules[2] also require such understanding.

One quantum effect connected with the KAM surface has been studied: Namely, a quantum system which at one time is localized entirely on one side of the KAM surface is at later times found in an exponential tunneling tail on the other side, whereas the classical system is strictly confined to one side of the surface.[3] This tunneling numerically shows a scaling dependence on Planck's constant h, and a relation to a more general theory of quantum scaling was suggested.[4] One motivation for us was to see how the quantum scaling is realized and relates to classical scaling. The renormalization theory of the critical KAM trajectory is a central achievement of this field.[5] It is found that the trajectory is approximated by a sequence of island chains, i.e., alternating elliptic and hyperbolic periodic orbits of period F_n, where $F_{n+1} = F_n + F_{n-1}$ is the Fibonacci sequence. The elliptic periodic points are surrounded by nearly integrable elliptic orbits (islands), while a stochastic region interpolates between the hyperbolic points along the separatrices with their homoclinic point structures. As $n \to \infty$ the chains geometrically converge to the KAM surface. For the case studied here, the kicked rotor at criticality, Fig. 1 a shows the critical KAM trajectory, and island chains at $F_n = 2$, 5, and 8 are shown as b, c, and d, respectively.

The quantum eigenstates (ES) are in fact associated not so much with the KAM trajectory as with its approximating island chains.[6] The left-hand side of Fig. 1 shows contour plots in the coherent-state representation of some ES which obviously correspond to classical or-

bits. The ES correspond to chains only up to some finite level $n(h)$, however. This maximum level can be estimated by equating the area of the stable region around an elliptic periodic point to h. This implies that finite h destroys the criticality of the transition.

Islands with $n < n(h)$ have a number of ES approximately equal to their area in units of h. They are like integrable harmonic oscillator ES and are labeled m below. In Fig. 1 b' the ES is $F_n = 2$, $m = 4$, for example.

There are also ES related to the hyperbolic points and their associated stochastic regions. In Fig. 1 e and f exhibit the classical stochastic orbits at periods 1 and 2; e' and f' show two ES. The ES are significant throughout the stochastic region, or more precisely, the part of the stochastic region associated with a given island chain. (Between chains there remain cantori which delay the passage of classical trajectories and impede quantum transport altogether.)

There is no sharp distinction between elliptic, "regular" ES and hyperbolic, "chaotic" ones, as there can be ES localized around the edges of the stable islands.
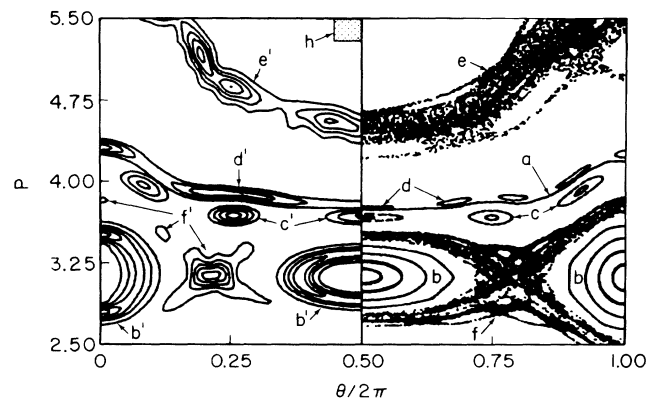

FIG. 1. Classical orbits (right-hand side) and quantum eigenstates (left-hand side) in phase space (angular momentum, angle/2π) for the kicked rotor at integer time. Planck's constant is chosen equal to the hatched area.

There are ES concentrated near the hyperbolic points, however, which are like ES in an inverted harmonic-oscillator potential. We have found some interesting properties of these ES, including an association with homoclinic points in the stochastic region, but we defer discussion of these points.[7] (The structures in Fig. 1 at e' and f' are related to the homoclinic points.)

The system we study is the periodically kicked rotor, the standard generic system. The Hamiltonian is $\mathcal{H} = \frac{1}{2}p^2 + \kappa \cos\theta \sum \delta(t-n)$, at $\kappa = \kappa_c = 0.971\,635\,406\,31$. In the quantum case, $p = -i\hbar\,\partial/\partial\theta$. The ES are of the period-1 unitary time evolution operator, $\mathcal{U}(1)$, with eigenvalues $e^{-i\omega_a}$ where $\hbar\omega_a$ is the quasienergy (QE). Our numerical technique is to start a wave packet in an interesting part of phase space, propagate it by a fast Fourier-transform method, and analyze the resulting time sequence, again by Fourier methods.[8] This method picks out just those ES important for the phase space reached by the packet, and has a direct classical interpretation. It typically gives 1 part in 10^4 accuracy, proportional to the length of the time series used.

To compare the ES with classical phase space, we employ the (Husimi) coherent-state representation (CSR). The CSR of state $|\psi\rangle$ is $|\langle\psi|p,\theta,\sigma\rangle|^2$, where $|p,\theta,\sigma\rangle$ is a Gaussian state of (angular) momentum width $\hbar\sigma$ centered at p,θ. The CSR is also a Gaussian smearing of the Wigner function. The Wigner function has many virtues, but it often oscillates violently instead of vanishing where the classical probability is small. The structures shown in Figs. 1 and 2 are at time $t = n$, "halfway through" a kick (rather than just after the kick as is customary), since then there is symmetry about $\theta = 0, \pi$.

Two of the periodic points under discussion at each n fall on the symmetry lines $\theta = 0, \pi$. On $\theta = \pi$ the periodic points are elliptic. They converge geometrically to the limit point $(p_c,\theta) = (3.737\,998\,30, \pi)$. Asymptotically $p_n - p_c \propto (\beta)^{-n}$ where $\beta = -3.066\,888\,2$. The θ dimension scales by a factor of $\alpha = -1.414\,836\,0$.

The map shown in Fig. 1 is called $z' = T(z)$, where $z = (p,\theta)$. Let $T(z,k)$ be $T(z)$ iterated k times. Scaling is formally the statement that the scaled iterated map $\Lambda^n T(\Lambda^{-n}z, F_n)$ is independent of n, for large n, where $\Lambda z = (\beta p, \alpha\theta)$ and the origin is taken at (p_c, π). Scaling only holds in a scaling region, $\mathcal{S}$, near (p_c, π). (Another such region, $\mathcal{S}'$, in on the line $\theta = 0$.)

The corresponding quantum map, $\mathcal{U}$, also scales[4] provided $\hbar$ is changed by the factor $\alpha\beta$. This is expressed in terms of the evolution operator $K(z,z',k,\hbar)$ of the Wigner function, $W(z,t,\hbar)$, where

$$W(z,t+k,\hbar) = \int d^2z'\, K(z,z',k,\hbar)W(z',t,\hbar).$$

The scaling is

$$\alpha\beta K(z,z',F_{n+1},\hbar) = K(\Lambda z, \Lambda z', F_n, \alpha\beta\hbar),$$

asymptotically, for z,z' in $\mathcal{S}$.

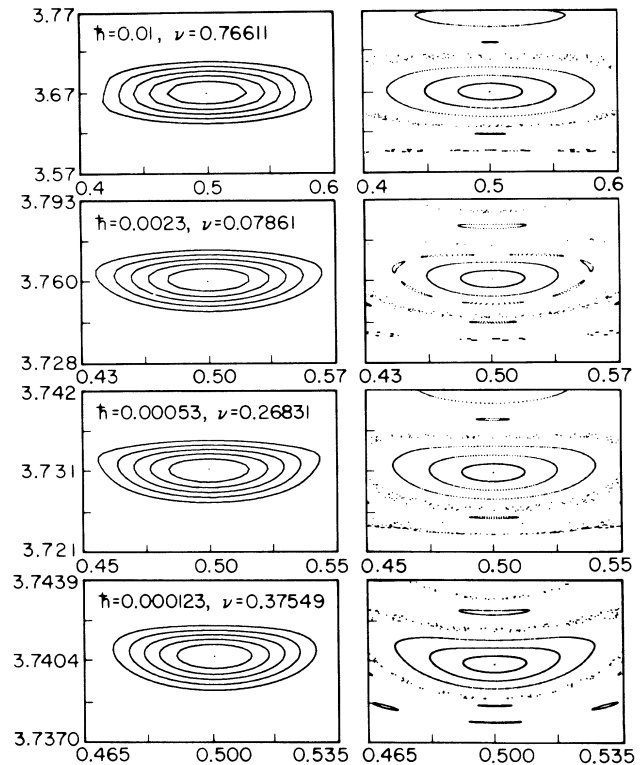Let P_n be a period F_n elliptic point in $\mathcal{S}$. If z is near

FIG. 2. Eigenstates (left-hand side) and orbits (right-hand side) near the period-5, -8, -13, and -21 elliptic points on the symmetry line $\theta = \pi$ which demonstrate scaling. Each picture is a blowup of part of the previous one, and $\hbar$ is also scaled on the left-hand side.

P_n, then $z' = T(z, F_n)$ is also near P_n. Correspondingly, for small $\hbar$ we find eigenstates of $\mathcal{U}(F_n)$ localized about P_n which have time-independent Wigner functions $W_{nm}(z,\hbar)$ with support in $\mathcal{S}$. The scaling relation above implies that the Wigner function of the period F_n state for Planck's constant $\hbar$ is the same as the scaled Wigner function of the period F_{n+1} state for $\hbar \to \hbar/\alpha\beta$, i.e., $W_{n+1,m}(z,\hbar) = \alpha\beta W_{nm}(\Lambda z, \alpha\beta\hbar)$. Further, an ES n,m will exist only for $\hbar$ less than some areas S_{nm} (approximately $1/m$th the island area). Then $S_{nm} = \alpha\beta S_{n+1,m}$.

Figure 2 shows such ES, for $F_n = 5$, 8, 13, and 21 ($m = 0$), scaled according to this prescription, and the corresponding classical orbits. On the classical side, one sees the higher-order orbit which is rescaled into the next picture down, but $\hbar$ is too large for this small area orbit to show on the quantum picture. (Technically, one has to introduce an added coordinate shear to get exact scaling.[5] We have not done this, so there is some distortion.)

Under $\mathcal{U}(k), k = 1 \ldots F_n - 1$, an ES ψ_0 localized near P_n is carried to a ES ψ_k localized about $T(P_n, k)$. The resulting F_n distinct ES are (nearly degenerate) ES of $\mathcal{U}(F_n)$ but not of $\mathcal{U}(1)$. They are easily superimposed, however, into ES of $\mathcal{U}(1)$ whose eigenvalues differ by the F_n'th roots of unity. Thus we may write the QE's of

$\mathcal{U}(1)$ as $E_{nmj} \cong E_n^0 + \hbar \omega_n (m + \frac{1}{2}) + jh/F_n$, for $h < S_{nm}$. For simplicity we adopt the harmonic approximation for states m, and $j = 1 \ldots F_n$ distinguishes ES degenerate under $\mathcal{U}(F_n)$.

Scaling applies to time-dependent Wigner functions and expectation values as well as those of ES. Time dependence comes from cross terms between distinct QE states making up a wave packet, and scaling, therefore, has implications for QE differences. In particular, it is clear that $F_n \omega_n \equiv F_r \omega_r \pmod{2\pi}$; that is, the fundmental QE differences of internal island ES are independent of island chain, when measured with scaled time and h. The QE E_n does not scale, however. When h is so small that E_r^0, E_n^0 are both defined, matrix elements between ES localized about P_r, P_n come only from tunneling effects smaller than any power of h. Any time-dependent part of a Wigner function depending on $E_n^0 - E_r^0$ is proportional to the ES overlap and vanishes classically. It is not expected to scale which is only proven to leading order in h.[4] (However, E_n^0 is the *classical* average QE over the F_n periodic points and the large n limit is approached geometrically with nontrivial exponent.)

The "hyperbolic" ES on chain n do not exhibit an F_n-fold degeneracy, nor do they scale. Indeed, lacking degeneracy, they can hardly scale since there are roughly F_n of them in the period F_n stochastic region, and F_n distinct ES would have to scale somehow into F_{n+1} distinct ES. However, wave packets starting in a scaling stochastic region $\mathcal{S}'$ must scale for the limited time that they remain in $\mathcal{S}'$. As before, this implies that the QE differences undergo an approximate scaling. One may produce a frequency spectrum, weighted by the probability of finding the corresponding ES, for a wave packet started in a hyperbolic scaling region. This spectrum must be approximately the same, up to a constant shift, for a scaled wave packet with scaled h. The spectrum [of $\mathcal{U}(5)$] for a wave packet started near the $F_n = 5$ hyperbolic point (in $\mathcal{S}'$) is compared in Fig. 3 with the spectrum [of $\mathcal{U}(21)$] of a scaled wave packet with rescaled h started near the period-21 points. The period-5 spectrum has been uniformly shifted to display the correspondence.

Evidently the two spectra are very similar and for large F_n would become continuous and identical. The scaling region becomes a smaller and smaller part of the whole period F_n stochastic region, and "hyperbolic" ES in the scaling region eventually escape to the "continuum" of nonscaling ES.

We next turn to the detailed mechanism by which the tunneling across the KAM trajectory occurs. It is numerically observed when an initial wave packet $|i\rangle$ (on one side of the KAM trajectory) is propagated forward in time that there is a long-term probability to find the ES $|f\rangle$, a wave packet on the opposite side of the KAM, even though classically that would be forbidden. Let the
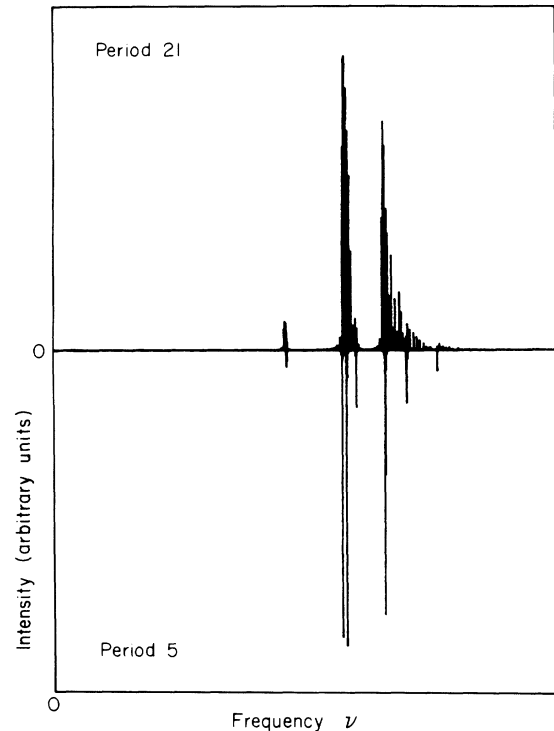

FIG. 3. Spectral analysis of wave packets, related by scaling, initiated on the hyperbolic points of period $F_n = 5$ (lower), and 21 (upper) at $\theta = 0$. The frequencies plotted are $E_a F_n / h \pmod{1}$ with E_a the QE. The period-5 points have been uniformly shifted.

"transport" amplitude be

$$\mathcal{M} = \langle f | \mathcal{U}(t) | i \rangle = \sum \langle f | \gamma \rangle \langle \gamma | i \rangle e^{-i\omega_\gamma t},$$

where $|\gamma\rangle$ is an ES of $\mathcal{U}$. If $|i\rangle$ and $|f\rangle$ are localized on opposite sides of the KAM trajectory, then the amplitude above is exponentially small. All ES $|\gamma\rangle$ will have exponentially small overlap with one or the other of $|i\rangle$ or $|f\rangle$. Thus the matrix elements come from an exponentially wide distribution, and typically one or a few ES $|\gamma\rangle$ will dominate the sum. When this happens, the amplitude evolves with a single frequency, and it is then easy to identify the ES $|\gamma\rangle$ which is of importance.

We remark that this situation occurs in conduction on disordered lattices with strongly localized electrons, where one or a few critical hoppings dominate the process for given parameters.[9] As in that case, we find large fluctuations of the transport $\mathcal{M}$ as the initial or final states or other parameters are changed.

In Fig. 4 a we reproduce the time average $\log_{10} |\mathcal{M}|^2$ found earlier.[3] In this case, $|i\rangle$ is a state of definite momentum ($p = 3.14$ at a time just after a kick), which happens to pass through the period-5 island chain below the KAM trajectory, and $|f\rangle$ is a state of definite momentum above the KAM trajectory whose value is the abscissa in Fig. 4.
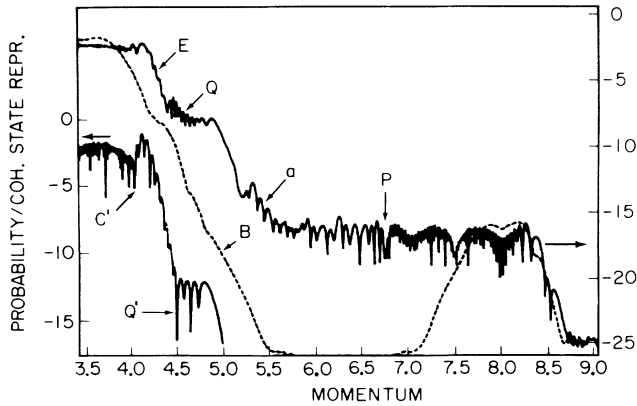
FIG. 4. Log$_{10}$ probability vs momentum (solid line, right-hand scale) long after the state is initiated with momentum $p = 3.14$ (on the other side of the KAM torus). B is the same, but with the angle required to be near π. The lower left gives the absolute square of a wave function vs momentum.

In the first exponential drop, Fig. 4 E, the dominant ES $|\gamma\rangle$ are (roughly five) of the ES associated with the period-5 chain. The exponential drop is just the tails of these ES. (Both elliptic and hyperbolic ES contribute, with the latter having somewhat longer tails.) A given ES tail is not really exponential, but is rather more Gaussian. However, over the relatively short range of momentum considered, and considering that the weight of ES contributing to Fig. 4 E changes substantially with p, the exponential approximation is fairly good. The absolute square of the momentum representation of one of these ES (Fig. 1 c') is shown in Fig. 4 c'.

The plateaus in Fig. 4 are associated with ES $|\gamma\rangle$ whose major weight is on the same side of the KAM as $|f\rangle$. The broad plateau P involves a single relatively extended ES $|\gamma\rangle$ belonging to a major chaotic region; in fact, just the ES shown in Fig. 1 e'. This can be determined by the time Fourier analysis of $\mathcal{M}$. To display this graphically, we have plotted in Fig. 4 B the $|\mathcal{M}|^2$ associated with the same initial state, but with $|f\rangle = |p,\pi, \sigma\rangle$. The "hole" in Fig. 4 B coincides with the elliptic period-1 region where the ES of Fig. 1 e' does not exist. The similar plateau Q belongs to "period 3" ES. (The structure Q' shown in the period 5 ES is a numerical error: We do not find the small tails of the ES with great accuracy and a bit of the wrong ES are mixed in. On the other hand, the small tails of $\mathcal{M}$ are found very accurately.) As h is made to decrease, plateaus appear and disappear and new pairs of ES dominate the transport, a feature connected with the large conductance fluctuation phenomenon mentioned before.

The tail E depends on h approximately as[3] $\exp(-pA/h^{1/3})$. It may be that the power $\frac{1}{3}$ is related to certain classical exponents.[4] If so, it requires that the tails of ES scale even though the ES themselves do not scale globally. Also, since Fig. 4 E really consists of a sequence

of drops with little plateaus, there has to be some scaling relation between these ES. We have found numerically that the small amplitude tails have an amazing knowledge of the classical phase-space structure. However, as mentioned, the evaluation of the distant tails of specific wave functions are numerically suspect and more work is needed to explain the result above.

In this work we have displayed quantum states corresponding to certain classical phase-space structures. If the classical structure scales, there is a quantum scaling as well. This results in scaling of some eigenstates, and of QE differences. Some light has been shed on the tunneling transport across KAM and cantori barriers, and effects reminiscent of conductance of localized electrons are encountered. Future work will address the association of quantum states with homoclinic orbits as well as questions involving KAM-type structures away from criticality.

[1]G. Casati, B. V. Chirikov, D. L. Sheplyansky, and I. Guarneri, Phys. Rev. Lett. **57**, 823 (1986); B. Blümel and U. Smilansky, Phys. Rev. Lett. **58**, 2531 (1986); K. A. H. van Leeuwen, G. v. Oppen, S. Renwick, L. B. Bowlin, P. M. Koch, R. V. Jensen, O. Rath, D. Richards, and J. G. Leopold, Phys. Rev. Lett. **55**, 2231 (1985).

[2]R. C. Brown and R. E. Wyatt, Phys. Rev. Lett. **57**, 1 (1986); M. J. Davis and J. K. Gray, J. Chem. Phys. **84**, 5389 (1986).

[3]T. Geisel, G. Radons, and J. Rubner, Phys. Rev. Lett. **57**, 2883 (1986), and Adv. Chem. Phys. **73**, 891 (1988).

[4]S. Fishman, D. R. Grempel, and R. E. Prange, Phys. Rev. A **36**, 289 (1987).

[5]J. M. Greene, J. Math. Phys. **9**, 760 (1968); S. J. Shenker and L. P. Kadanoff, J. Stat. Phys. **27**, 631 (1982); R. S. MacKay, thesis, Princeton University, 1982 (unpublished).

[6]S.-J. Chang and K.-J. Shi, Phys. Rev. A **34**, 7 (1986), and Phys. Rev. Lett. **55**, 269 (1985), have exhibited a number of eigenstates for this problem, and appear to suggest that there is a state associated with the KAM trajectory, which may be true within their numerical resolution. See also, G. P. Berman, O. F. Vlasova, and F. M. Izrailev, Zh. Eksp. Teor. Fiz. **93**, 470 (1987) [Sov. Phys. JETP **66**, 269 (1987)]; M. Toda and K. Ikeda, J. Phys. A **20**, 3833 (1987).

[7]G. Radons and R. E. Prange, to be published.

[8]D. R. Grempel, R. E. Prange, and S. Fishman, Phys. Rev. A **29**, 1639 (1984).

[9]See, for example, R. A. Webb, A. B. Fowler, A. Hartstein, and J. J. Wainer, Surf. Sci. **170**, 14 (1986).